Inorganic Chemistry
Communication

Inorg. Chem. 2010, 49, 4723–4725 4723
DOI: 10.1021/ic902182x

Microporous Lanthanide-Organic Frameworks with Open Metal Sites: Unexpected Sorption Propensity and Multifunctional Properties

Woo Ram Lee,[†] Dae Won Ryu,[†] Jin Wuk Lee,[†] Jung Hee Yoon,[†] Eui Kwan Koh,[‡] and Chang Seop Hong*[,†]

[†]*Department of Chemistry (BK21), Korea University, Seoul 136-713, Korea, and* [‡]*Nano-Bio System Research Team, Korea Basic Science Institute, Seoul 136-713, Korea*

Received November 4, 2009

Isostructural lanthanide-organic frameworks were prepared by a solvothermal reaction of the corresponding metal ions and the phosphine-oxide-based tricarboxylate ligand. The gravimetric gas uptake was unexpectedly increased when going from Nd^{3+} to Gd^{3+}, which is associated with the enhanced surface areas and electrostatic interactions between exposed metal ions and gas molecules with quadrupole moments.

Remarkable advances in metal−organic frameworks (MOFs) involve not only their emerging topologies, reminiscent of well-known zeolites or solid structures, but also their promising potential applications in areas such as gas storage,[1] separation,[2] and catalysis.[3] This diverse applicability is based on the fact that the porous frameworks have the merits of a high surface area and an adjustable pore size. Recently, MOFs have been introduced in biomedical applications such as cellular probes, drug storage and release as well.[4] The pursuit of multifunctional materials has also fueled the development of MOFs possessing a concomitant occurrence of a second trait or more.[5] Although lanthanide-based materials have been intensively studied in terms of magnetic and/or luminescent properties,[6] lanthanide-organic frameworks with permanent porosity have been less explored so far.[7] Provided that lanthanides exhibit magnetic and optical characters simultaneously, such lanthanide-based porous MOFs need to be more investigated in the search for exotic materials with more than dual functions.

In view of the hydrogen storage capabilities of microporous MOFs, particular attention has been paid to understand physisorption of diatomic hydrogen on the surfaces of MOFs. Experimentally, efficient methods to improve the hydrogen sorption affinities were reported; they include generation of exposed metal sites,[8] fabrication of catenation/interpenetration in coordination networks,[9] and spillover effect.[10] The open metal sites on the surfaces of MOFs that are usually formed by removing coordinate solvent molecules on evacuation or photolysis confers high binding energies of metal ion−H_2 compared to the traditional ones.[11] To account for gas adsorption results of MOFs or to seek optimal gas uptake conditions, several theoretical investigations have been carried out suggesting that binding strengths of gas molecules depend on dispersion forces and electrostatic interactions.[12] It is thus believed that exposed metal ions in porous coordination materials can strongly correlate with gas molecules bearing dipole and/or quadrupole moments. To gain insight into gas uptake capacities contributed from electrostatic terms between exposed metal ions and gas molecules, it is therefore highly desirable to devise isostructural MOFs in which gas sorption is systematically affected by constituent metal ions with different charge densities.

*To whom correspondence should be addressed. E-mail: cshong@korea.ac.kr.

(1) (a) Chen, B.; Ockwig, N. W.; Millward, A. R.; Contrras, D. S.; Yaghi, O. M. *Angew. Chem., Int. Ed.* **2005**, *44*, 4745. (b) Ma, S.; Sun, D.; Simmons, J. M.; Collier, C. D.; Yuan, D.; Zhou, H.-C. *J. Am. Chem. Soc.* **2008**, *130*, 1012.
(2) Matsuda, R.; Kitaura, R.; Kitagawa, S.; Kubota, Y.; Belosludov, R. V.; Kobayashi, T. C.; Sakamoto, H.; Chiba, T.; Takata, M.; Kawazoe, Y.; Mita, Y. *Nature* **2005**, *436*, 238.
(3) (a) Horike, S.; Dincă, M.; Tamaki, K.; Long, J. R. *J. Am. Chem. Soc.* **2008**, *130*, 5854. (b) Seo, J. S.; Whang, D.; Lee, H.; Jun, S. I.; Oh, J.; Jeon, Y. J.; Kim, K. *Nature* **2000**, *404*, 982.
(4) (a) Horcajada, P.; Serre, C.; Maurin, G.; Ramsahye, N. A.; Balas, F.; Vallet-Regi, M.; Sebban, M.; Taulelle, F.; Ferey, G. *J. Am. Chem. Soc.* **2008**, *130*, 6774. (b) Taylor-Pashow, K. M. L.; Rocca, J. D.; Xie, Z.; Tran, S.; Lin, W. *J. Am. Chem. Soc.* **2009**, *131*, 14261. (c) An, J.; Geib, S. J.; Rosi, N. L. *J. Am. Chem. Soc.* **2009**, *131*, 8376.
(5) Ouellette, W.; Prosvirin, A. V.; Whitenack, K.; Dunbar, K. R.; Zubieta, J. *Angew. Chem., Int. Ed.* **2009**, *48*, 2140.
(6) (a) Chen, B.; Wang, L.; Zapata, F.; Qian, G.; Lobkovsky, E. B. *J. Am. Chem. Soc.* **2008**, *130*, 6718. (b) Chandler, B. D.; Yu, J. O.; Cramb, D. T.; Shimizu, G. K. H. *Chem. Mater.* **2007**, *19*, 4467. (c) Ma, S.; Yuan, D.; Wang, X.-S.; Zhou, H.-C. *Inorg. Chem.* **2009**, *48*, 2072. (d) Zhao, B.; Chen, X.-Y.; Cheng, P.; Liao, D.-Z.; Yan, S.-P.; Jiang, Z.-H. *J. Am. Chem. Soc.* **2004**, *126*, 15394.
(7) Devic, T.; Serre, C.; Audebrand, N.; Marrot, J.; Férey, G. *J. Am. Chem. Soc.* **2005**, *127*, 12788.
(8) (a) Dincă, M.; Han, W. S.; Liu, Y.; Dailly, A.; Brown, C. M.; Long, J. R. *Angew. Chem., Int. Ed.* **2007**, *46*, 1419. (b) Caskey, S. R.; Wong-Foy, A. G.; Matzger, A. J. *J. Am. Chem. Soc.* **2008**, *130*, 10870. (c) Zhou, W.; Wu, H.; Yildirim, T. *J. Am. Chem. Soc.* **2008**, *130*, 15268. (d) Ma, S.; Yuan, D.; Chang, J. S.; Zhou, H.-C. *Inorg. Chem.* **2009**, *48*, 5398.
(9) Ma, S.; Sun, D.; Ambrogio, M.; Fillinger, J. A.; Parkin, S.; Zhou, H.-C. *J. Am. Chem. Soc.* **2007**, *129*, 1858.
(10) Cheon, Y. E.; Suh, M. P. *Angew. Chem., Int. Ed.* **2009**, *48*, 2899.
(11) Kaye, S. S.; Long, J. R. *J. Am. Chem. Soc.* **2008**, *130*, 806.
(12) (a) Lochan, R. C.; Head-Gordon, M. *Phys. Chem. Chem. Phys.* **2006**, *8*, 1357. (b) Zhou, W.; Yildirim, T. *J. Phys. Chem. C* **2008**, *112*, 8132.

Published on Web 05/07/2010

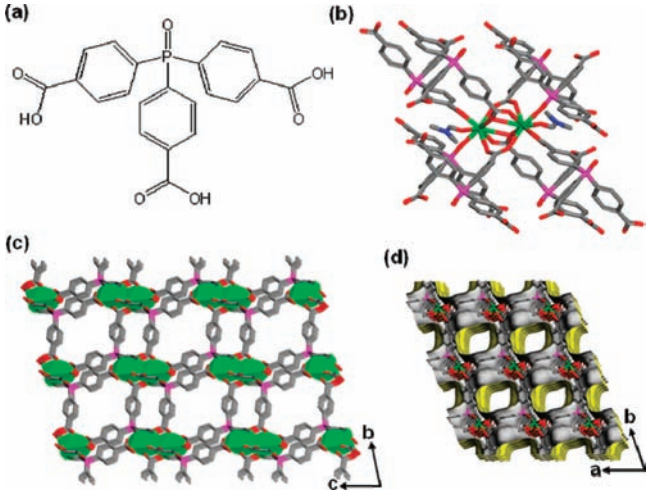

Figure 1. (a) H_3TPO ligand and (b) molecular view of the SBU in **1** including coordinated DMF molecules. (c) Extended network structure of **1** shown in the *bc* plane, in which the SBUs are represented in a polyhedron shape. (d) Top view of 1D channels in the *ab* plane.

In this communication, we present the syntheses, structures, sorption, and optical and magnetic properties of four 3D networks [Ln(TPO)] [Ln^{3+} = Nd (**1**), Sm (**2**), Eu (**3**), Gd (**4**); H_3TPO = tris-(4-carboxylphenyl)phosphineoxide]. Charges and radii of the Ln ions play a key role in electrostatic sorbate−sorbent interactions, which may be responsible for the unexpected increased amount of gravimetric gas sorption when moving from Nd to Gd.

A solvothermal reaction of $Ln(NO_3)_3 \cdot xH_2O$ and H_3TPO in a mixed solvent of DMF/H_2O/MeOH (3:3:1 v/v), together with the addition of a small amount of neat HNO_3, produced solvated crystalline products. It is essential to maintain the acidic conditions by adding HNO_3 for the formation of the target frameworks. The other isostructural Ln series beyond Gd were not isolated under the same experimental conditions.

All complexes crystallized in the triclinic system with the space group $P\bar{1}$. Because they are isostructural, the structure of **1**-DMF is representively described. The crystal structure of **1**-DMF consists of a 3D network (Figure 1). The central Nd atom is surrounded by nine neighboring oxygen atoms from eight TPO ligands and one coordinated DMF molecule. The two Nd centers are quadruply bridged by four carboxylates of TPOs, leading to the construction of a secondary building unit (SBU) acting as an 8-connected node. In the network, the phosphine oxide-O can form an even stronger bond to Nd, with a shortest Nd−O bond length of 2.385(3) Å, than the other Nd−O bond distances in the range 2.404(3)−2.791(3) Å. This feature is different from the TPO-based Zn coordination polymer where a very weak bond interaction between phosphine oxide and Zn is established.[13] The P−O bond length of 1.496(3) Å is in the usual scope for the polar nature of the moiety.[14] A close inspection of the solvent-accessible surface discloses that straight open channels are present along the crystallographic axes. The passage windows in **1** are estimated to be 4.9 × 6.4 $Å^2$, 3.8 × 4.9 $Å^2$, and 3.4 × 4.4 $Å^2$, after taking into account the van der Waals surface of the backbone. The effective aperture sizes for **2**−**4** are almost similar to those for **1** (Figure S1, Supporting Information). The solvent accessible void volume calculated by PLATON[15] is alike, 48.4% for **1**, 48.7% for **2**, 48.2% for **3**, and 49.0% for **4**.

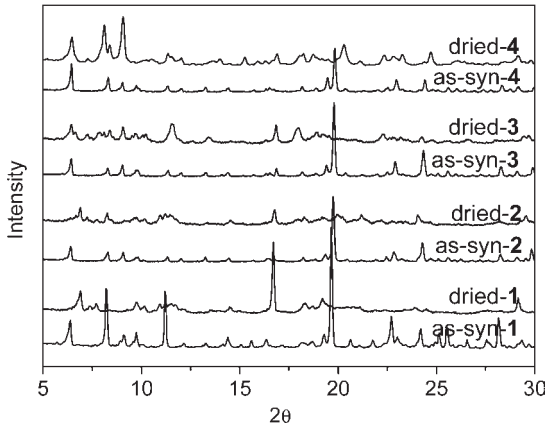

Figure 2. PXRD patterns of as-synthesized and dried samples of **1**−**4** under the best desolvated conditions.

Thermogravimetric analysis on the as-prepared form of **1** indicated a weight loss of 25.0% in the temperature range 27−265 °C, which is consistent with the decomposition of all lattice solvents (two H_2O and one DMF) and one coordinated DMF molecule (24.8%). The framework is thermally quite stable up to 500 °C, which is comparable to that of the coordinatively linked Yb MOF and much higher than those (< 400 °C) in 3D-metal-based MOFs.[16,17] The other samples also displayed analogous thermal stabilities (Figures S2 and S3, Supporting Information). The desolvated samples **1**−**4** were prepared by solvent exchange in chloroform for one day and heated under a vacuum at 80, 100, 160, 180, and 240 °C for 20 h. PXRD was taken to confirm the structural integrity (Figures 2 and S4, Supporting Information) and show the structural changes in drying processes. The complete elimination of the coordinated DMF molecule in the complexes after activation processes was checked by the IR spectra where the characteristic C=O stretchings of DMF disappeared in the desolvated samples (Figure S5, Supporting Information). The best evacuation conditions were found at 160 °C for **1**−**3** and 180 °C for **4**, which were tested by measuring the N_2 uptake of the desolvated solids activated at different temperatures (Figure S6, Supporting Information).

The N_2 sorption isotherms at 77 K for **1**−**4** are illustrated in Figure 3a, showing typical type I behavior without hysteresis and thus ensuring permanent microporosity. The Brunauer−Emmett−Teller (BET) surface areas for **1**−**4** are 793, 994, 1079, and 1163 m^2/g, and the total pore volumes for **1**−**4** are 0.344, 0.425, 0.456, and 0.487 cm^3/g, respectively. For H_2 uptake (Figure 3b), the maximum amounts for **1**−**4** at 1 atm and 77 K reach to 0.89 wt % (100 cm^3/g), 1.02 wt % (134 cm^3/g), 1.52 wt % (170 cm^3/g), and 1.82 wt % (208 cm^3/g), respectively. The number of H_2 molecules per formula unit

(13) Humphrey, S. M.; Oungoulian, S. E.; Yoon, J. W.; Hwang, Y. K.; Wise, E. R.; Chang, J.-S. *Chem. Commun.* **2008**, 2891.
(14) Engelhardt, L. M.; Raston, C. L.; Whitaker, C. R.; White, A. H. *Aust. J. Chem.* **1986**, *39*, 2151.
(15) Spek, A. L. *PLATON, A Multipurpose Crystallographic Tool*; Utrecht University: The Netherlands, 2005.
(16) Ma, S.; Wang, X.-S.; Yuan, D.; Zhou, H.-C. *Angew. Chem., Int. Ed.* **2008**, *47*, 4130.
(17) (a) Chun, H.; Dybtsev, D. N.; Kim, H.; Kim, K. *Chem.—Eur. J.* **2005**, *11*, 3521. (b) Zou, Y.; Hong, S.; Park, M.; Chun, H.; Lah, M. S. *Chem. Commun.* **2007**, 5182.

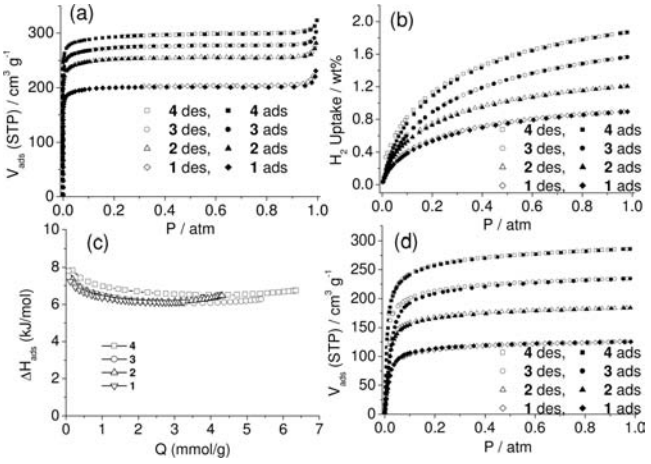

Figure 3. Gas sorption isotherms of (a) N_2, (b) H_2, and (d) CO_2 for the porous frameworks **1**−**4**: ads = adsorption, des = desorption. (c) Isosteric heats of adsorption of H_2.

is prone to gradually alter from 2.5 for **1** to 5.9 for **4**. When the density of liquid hydrogen at 20 K and 1 atm (0.0708 g/mL) is considered, the filling of H_2 in the frameworks is 35% of the total pore volume for **1**, 40% for **2**, 47% for **3**, and 54% for **4**. We measured additional hydrogen isotherms at 87 K to determine isosteric heats of adsorption derived from the Clausius−Clapeyron equation (Figures 3c and S7, Supporting Information).[18] At low coverage in which H_2-open metal site interactions are assumed, the adsorption enthalpy spans from 7.1 kJ/mol for **1** to 7.8 kJ/mol for **4**. The obtained values are similar to those of metal−organic or metal−cyanide frameworks.[19]

Because all compounds have identical structures and nearly the same portal sizes for entering guest molecules, it is reasonably expected that, as the atomic number of lanthanides increases from Nd^{3+} (**1**) to Gd^{3+} (**4**) and the molecular mass becomes heavier, gravimetric gas adsorption tends to gradually diminish. This is why there has been a special emphasis on porous coordination frameworks with lightweight elements such as Mg^{2+} in recent investigations on MOFs, with the aim of increasing H_2 storage.[20] However, this prediction is sharply contrary to the current observation of the H_2 sorption capacities. This trend can be mainly understood in terms of the BET surface areas of the dried samples as already well revealed in microporous MOFs.[21]

Moreover, it is informative to examine the sorption behaviors on the other aspect. As summarized in Table S1 (Supporting Information), when going from Nd^{3+} to Gd^{3+}, R_{Ln3+} undergoes a steady reduction, and subsequently the charge density (charge/R_{Ln3+}) becomes pronounced. The removal of the bound DMF molecules gives rise to open metal sites, which are important in increasing binding strengths between frameworks and guest molecules. The electrostatic interactions between the field gradient induced partially from the charge density of Ln^{3+} and the quadrupole moment of H_2 give some additional impact on the unusual H_2 uptake propensity, because, conversely, polarizabilities, which affect dispersion potentials, decrease with increasing atomic number of lanthanide elements.[22,23] The similar effects of cation charge and ionic radius on gas sorption were also demonstrated in zeolites with alkali cations.[12,24]

To further probe the role of the charge density, we performed the CO_2 sorption experiments at 195 K because this linear molecule has a larger quadrupole moment than H_2.[22] As seen in Figure 3d, the CO_2 uptake increases from 125.3 cm^3/g for **1** to 285.8 cm^3/g for **4**, in good agreement with the variation of the H_2 adsorption. The H_2 sorption capacity of **4** is 2.1 times larger than that of **1**, whereas the ratio of **4** to **1** in the CO_2 sorption is 2.3. This difference in the gas uptake may arise from the greater quadrupole moment of CO_2. In comparison, the Ar gas without quadrupole moment was adsorbed (Figure S8, Supporting Information) and the ratio is 1.2, significantly smaller than the other gases with quadrupole moments. This suggests that the charge density partly contributes to the improved gas uptake together with the BET surface areas.

The emission spectrum of the solvated form of **3**, excited by ultraviolet light, shows well-defined transitions (Figures S9 and S10, Supporting Information). In magnetic properties (Figure S11, Supporting Information), for the solvated phases of **1**−**3**, the reduction in χT upon cooling may be pertinent to the depopulation of excited states and possible magnetic couplings.[25] A best fit of the solvated **4** to the dimer model ($H = -JS_{Gd1} \cdot S_{Gd2}$) gives $g = 1.97$ and $J = 0.031$ cm^{-1}.

In summary, we have prepared and characterized four isostructural lanthanide-organic frameworks incorporated with phosphine oxide-based tricarboxylate. The sorption properties indicate that the gas adsorption increases when moving from Nd^{3+} to Gd^{3+}. This observation is related to the enhanced BET surface areas and charge density.

Acknowledgment. This work was supported by the Korea Research Foundation Grant funded by the Korean Government (MEST) (KRF-2009-220-C00021) and also by PAL (2009-1063-10).

Supporting Information Available: X-ray crystallographic file in CIF format; additional synthetic, structural, luminescent, and magnetic data for **1**−**4**. This material is available free of charge via the Internet at http://pubs.acs.org.

(18) Rouquerol, F.; Rouquerol, J.; Sing, K. *Adsorption by Powders and Porous Solids*; Academic Press: London, 1998.
(19) Murray, L. J.; Dincă, M.; Long, J. R. *Chem. Soc. Rev.* **2009**, *38*, 1294.
(20) Dincă, M.; Long, J. R. *J. Am. Chem. Soc.* **2005**, *127*, 9376.
(21) Wong-Foy, A. G.; Matzger, A. J.; Yaghi, O. M. *J. Am. Chem. Soc.* **2006**, *128*, 3494.
(22) Stogryn, D. E.; Stogryn, A. P. *Mol. Phys.* **1966**, *11*, 371.
(23) Yang, R. T. *Adsorbents: Fundamentals and Applications*; John Wiley & Sons, Inc.: New York, 2003.
(24) (a) Barrer, R. M. *Zeolites and Clay Minerals*; Acadimic Press: New York, 1978. (b) Barrer, R. M.; Gibbons, R. M. *Trans. Faraday Soc.* **1965**, *61*, 948.
(25) Wan, Y.; Zhang, L.; Jin, L.; Gao, S.; Lu, S. *Inorg. Chem.* **2003**, *42*, 4985.